

New Polar Phases of 1,4-Diazabicyclo[2.2.2]octane Perchlorate, An NH⁺⋯N Hydrogen-Bonded Ferroelectric

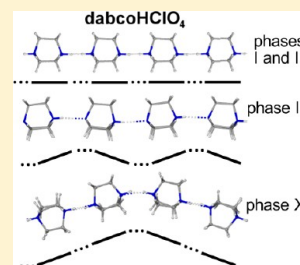
Anna Olejniczak,[†] Michalina Anioła,[†] Marek Szafranski,^{*‡} Armand Budzianowski,[†] and Andrzej Katrusiak^{*‡}

[†]Faculty of Chemistry, Adam Mickiewicz University, Umultowska 89b, 61-614 Poznań, Poland

[‡]Faculty of Physics, Adam Mickiewicz University, Umultowska 85, 61-614 Poznań, Poland

S Supporting Information

ABSTRACT: Exceptionally rich diagram of ten phases, I–X, has been revealed for ferroelectric 1,4-diazabicyclo[2.2.2]octane perchlorate, [C₆H₁₃N₂]⁺ClO₄[−], dabcoHClO₄. Pressure- and temperature-induced transformations of this NH⁺⋯N hydrogen bonded structure have been characterized by single-crystal X-ray diffraction, calorimetric, and dielectric measurements. At high pressure the single crystals were in situ grown in a diamond-anvil cell at isochoric conditions. There are nine phases of dabcoHClO₄ between 400 and 11 K at ambient pressure, whereas phase X is formed at 1.5 GPa and 296 K. Tetragonal phase I space group *P4/mmm* transforms to orthorhombic phases II (*Pm2₁n*), III (*Pc2₁n*), IV (*Pc2a*), and V (orthorhombic-modulated) on decreasing temperature. Phase II is stable up to 0.22 GPa, at 0.6 GPa phase III is formed, and above 1.50 GPa a new phase X (*Pc2₁a*) has been obtained. At normal conditions dabcoHClO₄ is isostructural with the ferroelectric crystal of dabcoHBF₄; however, their phase diagrams are very different. Above 1.8 GPa dabcoHClO₄ cocrystallizes with solvate molecules.



1. INTRODUCTION

1,4-Diazabicyclo[2.2.2]octane (dabco) forms with mineral acids a fascinating group of monosalts of exceptional dielectric properties. These monosalts can be described by a general formula dabcoHX, where X = Br[−], I[−], ClO₄[−], BF₄[−], and ReO₄[−]. At normal conditions in the monosalts structures, the dabcoH⁺ cations are NH⁺⋯N bonded into linear chains. DabcoHClO₄ and dabcoHBF₄ are ferroelectric, with the spontaneous polarization is perpendicular to the NH⁺⋯N-bonded chains.^{1–4}

In dabco perchrenate⁵ (dabcoHReO₄), the spontaneous polarization is nearly parallel to the NH⁺⋯N bonds, despite a considerable similarity to the dabcoHClO₄^{1,2,6,7} and dabcoHBF₄^{1–4,8} structures. Furthermore, it was found that dabco hydriodide (dabcoHI) and dabco hydrobromide (dabcoHBr) exhibit anisotropic ferroelectric relaxor properties, where the giant dielectric response is observed along the NH⁺⋯N hydrogen bonds only.^{9–12} Much weaker relaxor properties along the NH⁺⋯N-bonded chains were evidenced in dabcoHBF₄, too.³ The structural origin of the different behaviors of structurally similar crystals remains unclear. It was found, that the dabcoHX complexes are prone to exist in polymorphic forms. For example, ten polymorphs have been evidenced so far for dabcoHI at different conditions of temperature and pressure.¹⁰ However, except for polymorph V of dabcoHI, isostructural to dabcoHBr phase II, their other phases are drastically different in their structures and properties. Thus, we have continued the study of dabcoHClO₄ in varied pressure and temperature to establish if new polymorphs, such as the ferroelectric phases of dabcoHReO₄,¹³ can be obtained. Pressure can considerably modify the structure of NH⁺⋯N-bonded compounds. For example, in all dabcoHI polymorphs,

the NH⁺⋯N-bonded chains of dabcoH⁺ cations are retained, whereas in dabcoHBr only phase III is NH⁺⋯N-bonded (and isostructural with relaxor phase V of dabcoHI).^{11,14} Phase II of presently investigated ferroelectric dabcoHClO₄ is isostructural with phase II of dabcoHBF₄; the space-group symmetry of both crystals in phase II is the same, the positions of cationic chains and anions is very similar and the protons are ordered. DabcoHBF₄ exhibits a most intriguing transition to low-temperature phase III, where on lowering temperature below 153 K the protons become disordered in NH⁺⋯N bonds. However, it is shown below that on lowering temperature the structure of dabcoHClO₄ is modified differently than it was previously observed in dabcoHBF₄.^{1–4,8} The detailed description of structure–property relations and transformations of NH⁺⋯N bonds in ionic crystals and NH⋯N bonds in molecular^{15–17} crystals is essential for efficient search for new ferroelectric and relaxor materials.

2. EXPERIMENTAL METHODS

2.1. Calorimetry. Differential scanning calorimetry (DSC) and dielectric spectroscopy were used for detecting the phase transformations in dabcoHClO₄. The DSC measurements were carried out on a Q2000 (TA Instruments) calorimeter. A polycrystalline sample was heated/cooled at a rate of 10 K/min. The indium standard was used for the temperature and enthalpy calibrations.

Dielectric measurements were performed on the pressed pellets with painted silver electrodes, at ambient pressure and at hydrostatic

Received: February 18, 2013

Revised: April 24, 2013

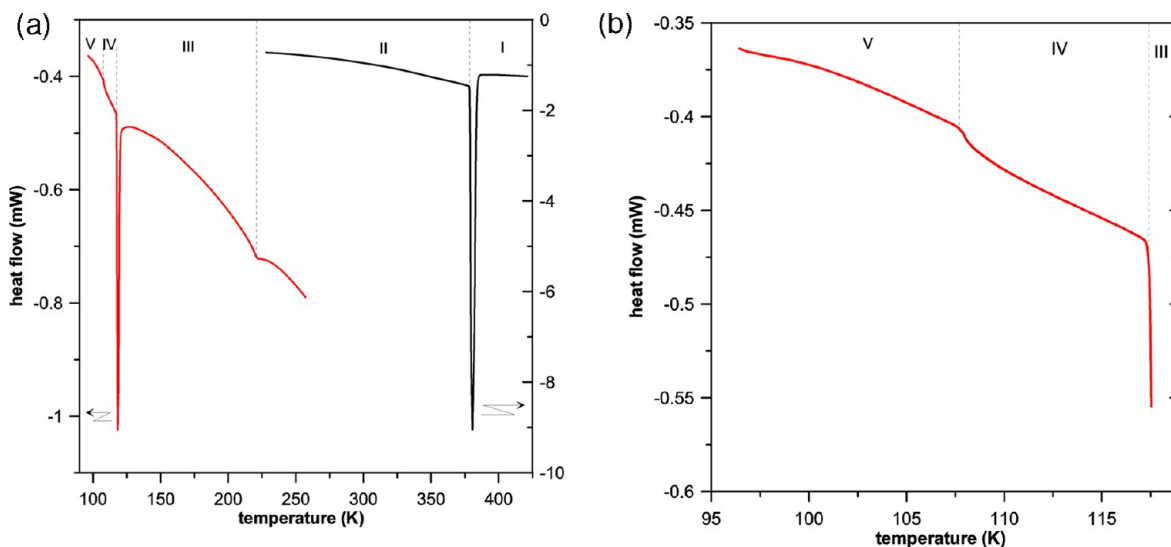


Figure 1. DSC heating run across the phase transition boundaries: (a) in the temperature range 100–420 K and (b) enhanced DSC heating run in the temperature range 95–120 K. Different scales were applied to show the details in the low temperature range. Because of the temperature limit of the apparatus and the temperature hysteresis of the transition between phases IV and V the associated thermal anomaly could be observed only during the sample heating. The vertical dashed lines mark the transition points and the Roman numbers label the phases.

pressures up to 0.6 GPa. Measurements of the relative complex electric permittivity $\epsilon = \epsilon' - i\epsilon''$ were carried out in the frequency range from 1 kHz to 3 MHz with a Hewlett-Packard 4192A impedance analyzer. The amplitude of the ac measuring electric field was of 3–5 V/cm. The temperature of the samples was changed at a rate ranging from 0.5 to 1 K/min. A closed-cycle cooler CCC1204 (Oxford Instruments) was used for the low-temperature measurements down to 11 K. For high-pressure dielectric studies the samples were mounted in a beryllium–copper cell ensuring the pressure range to 1 GPa. The cell was made in a form of 135 mm length drilled cylinder. The outside and inside diameters were of 48 and 13 mm, respectively. The cell was closed with two plugs, one connected to a high-pressure tube and the second one equipped with electrical leads. Helium was used as the medium transmitting pressure from a gas compressor U11 (Unipress) to the cell. The pressure was calibrated by means of a manganin gauge with an accuracy of ± 3 MPa and the temperature was controlled directly inside the cell by a copper-constantan thermocouple.

The thermal anomalies in DSC signal (Figure 1), apparent in the heating run, indicate that in the temperature range between 100 and 400 K the crystal undergoes a sequence of four phase transitions. Apart from the first-order ferroelectric-to-paraelectric phase transition at $T_{21} = 378$ K, described earlier,¹ a continuous phase transition at $T_{32} = 220$ K, as well as two first-order phase transitions at $T_{43} = 116$ K and $T_{54} = 107$ K (the subscript indices are two numbers of transforming phases), are observed. These transitions have been confirmed by anomalies in the temperature dependence of electric permittivity, plotted in Figure 2. The first-order character of the transition between phases IV and V is apparent from the DSC signal shape, quite different than the shape of signals of second-order transitions. As shown in Figure 1b, the DSC signal deflects from the baseline at T_{54} , while for a clear second-order (continuous) phase transition, like between phases III and II, the DSC-signal anomalous part starts well below the transition point, and then it returns to the baseline level above T_{32} . Most importantly, the first-order character of the transitions between phases V–IV and IV–III was unambiguously demonstrated by the presence of thermal hysteresis between the cooling and heating runs.

Furthermore, below 100 K the dielectric response of the crystal shows four additional anomalies corresponding to the phase transitions observed on heating at $T_{65} = 95$ K (probably first-order), $T_{76} = 76$ K (first-order), $T_{87} = 57$ K (first-order), and $T_{98} = 46$ K (second-order). Thus, the calorimetric and dielectric experiments indicate that at ambient pressure dabcoHClO₄ exhibits an exceptional richness of nine crystalline phases. The pressure dependence of phase

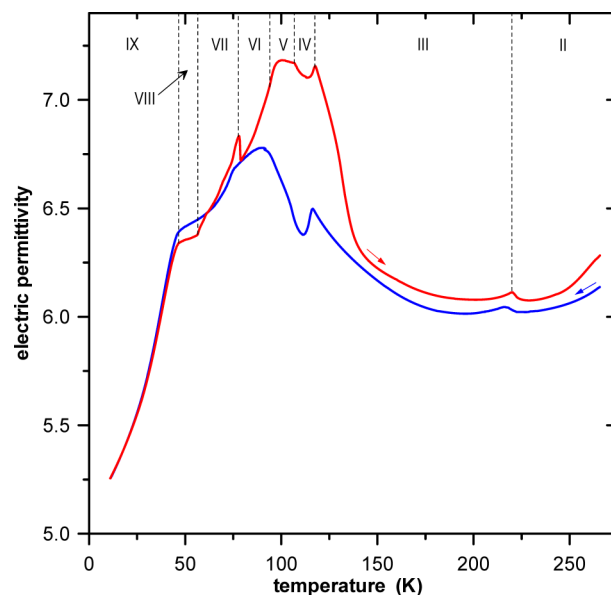


Figure 2. Real part of electric permittivity, ϵ' , measured at the 100 kHz frequency on cooling and heating the polycrystalline sample, as indicated by arrows. The phase boundaries corresponding to the dielectric anomalies are marked by vertical dashed lines.

boundaries above 80 K has been examined by electric permittivity measurements. The evolution of the dielectric response of the crystal at elevated pressures is shown in Figure 3.

2.2. Crystal Growth at High Pressure. The high-pressure diffraction experiments on dabcoHClO₄ were performed on the samples in situ crystallized in a modified high-pressure diamond anvil-cell (DAC),¹⁸ with the anvils directly supported on steel backing plates.¹⁹ Pressure in the DAC chamber was calibrated by the ruby-fluorescence method,^{20,21} with a Photon Control spectrometer, affording the accuracy of 0.02 GPa; pressure was calibrated before and after each diffraction measurement. The in situ crystallizations of dabcoHClO₄ were performed from the solutions in methanol, in methanol/water mixture (1:1), and in methanol/ethanol/water (16:3:1). Three forms of dabcoHClO₄ were grown at high-pressure isochoric conditions below 2 GPa. The DAC chamber was filled with

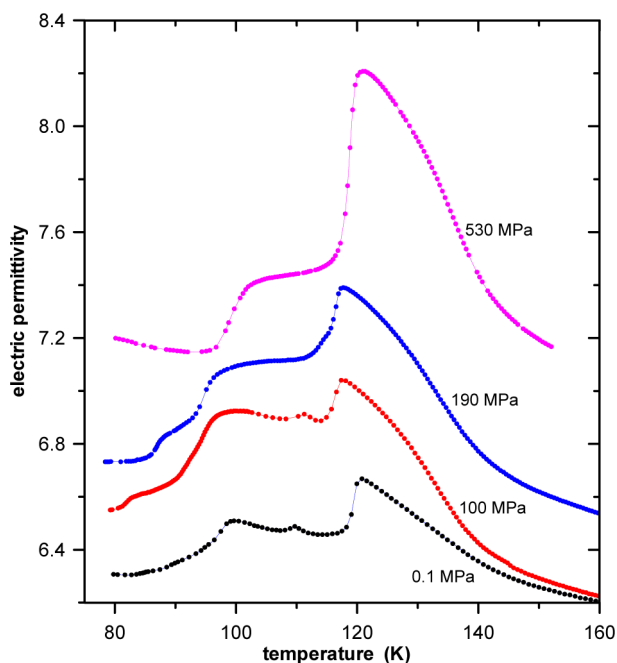


Figure 3. Pressure-induced changes in the dielectric response of dabcoHClO₄, measured in the heating runs at the 1 MHz frequency, in the temperature range 80–160 K. The subsequent high-pressure curves measured at 100, 190, and 530 MPa were shifted upward respectively by 0.2, 0.2, and 1.1 to avoid the overlapping.

the solution and the compound. Alternatively, after placing some grains of dabcoHClO₄ in the chamber and topping it up with the solvent, the DAC was sealed and pressure was increased. Then the DAC was heated up till all crystals dissolved. After a single crystal nucleated, it was grown by slowly cooling the DAC (Figures 4–6). At 1.80 GPa and 373 K, the crystal grew in the form of a needle, however below 343 K several other needles grew nearly parallel to the first one

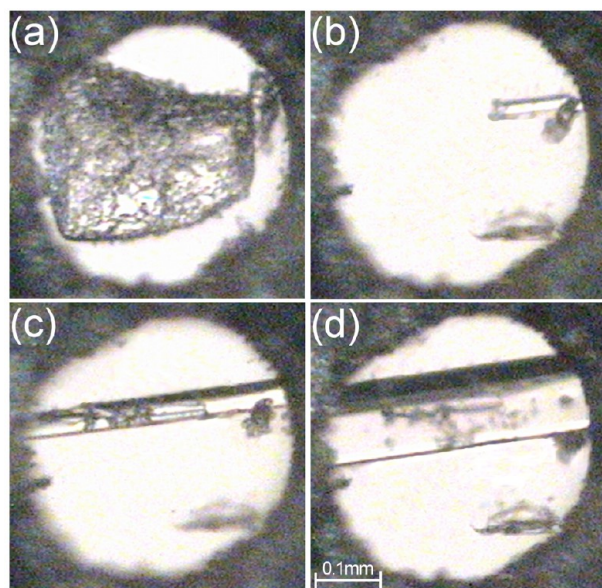


Figure 4. Preparation of dabcoHClO₄ single crystal in phase II in the DAC chamber by isochoric growth from methanol solution: (a) a crystal of dabcoHClO₄ submerged in methanol at 0.20 GPa/296 K, (b) a seed nucleated at 373 K after dissolving the sample at 383 K, (c) 353 K, and (d) at 0.20 GPa/296 K. Two small ruby chips for pressure calibration lie close to the right and bottom-right edge of the gasket.

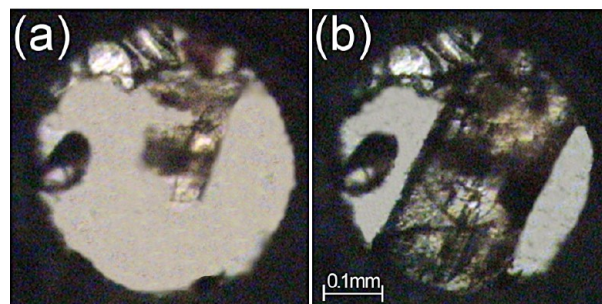


Figure 5. Methanol solution of dabcoHClO₄ sealed in the DAC chamber (a) and (b) the single crystal in phase III at 1.0 GPa/296 K. Four chips of ruby are located close to the left and top parts of the gasket.

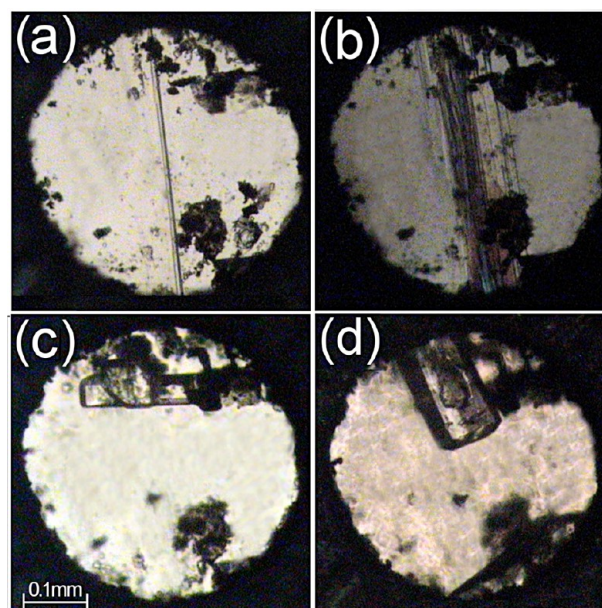


Figure 6. DabcoHClO₄ crystal in phase X grown from methanol/water 1:1 solution: (a) a needle seed at 373 K, (b) several needles at 343 K, (c) another crystal nucleated at 393 K, and (d) three single crystals lying at the top, right and bottom edges of the chamber at 1.80 GPa/296 K. Several chips of ruby powder for pressure calibration are scattered in the chamber.

(Figure 6b). Therefore the sample was dissolved again by heating it to 393 K and three seeds in a new form X appeared (Figure 6c). When cooled below 393 K, one of them dissolved and two others continued to grow (Figure 6d). It can be noted that the needle shape of the crystals in Figure 6a and 6b is different than those shown in Figure 6c and 6d; the latter are elongated parallelepipeds. According to their morphology, it appears that the crystals in Figure 6a and 6b are of a different phase than all other phases characterized in this study. However, the needle-shaped crystals (Figures 6a and 6b) were too small for X-ray diffraction measurement by using a sealed tube in our laboratory. All our attempts to perform crystallization of dabcoHClO₄ above 1.8 GPa were hampered by the formation of solvates with the solvent molecules.

2.3. X-Ray Diffraction Analysis. The single-crystal data have been measured with a KUMA KM4-CCD diffractometer. The CrysAlis software²² was used for the data collections²³ and preliminary reduction of data; the reflections overlapping with diamond reflections were eliminated and intensities were corrected for the sample and the DAC absorption and for the sample shadowing by the gasket.^{24,25} For the low-temperature measurements, an Oxford Cryosystems 700 Series attachment was used. The structures of phases II (at 0.20 GPa/

296 K, III (at 1.00 GPa/296 K) and X (1.80 GPa/296 K) were solved straightforwardly by direct methods and refined by full-matrix least-squares.²⁶ Anisotropic temperature factors were generally applied for all non-hydrogen atoms, except that isotropic thermal parameters retained for few atoms refining to unreasonably elongated thermal ellipsoids. The ethylene H-atoms were located from molecular geometry ($d_{C-H} = 0.97 \text{ \AA}$) and their U_{iso} values constrained to $1.2 \cdot U_{eq}$ of the carrier atoms. The amine protons were either located from the difference Fourier maps (low-temperature phase III), or introduced at ideal positions at both nitrogen atoms ($d_{N-H} = 0.86 \text{ \AA}$) with their $U_{iso} = 1.2U_{eq}$ of the nitrogen and then their partial site occupation (SOF) at N1 and N2 was refined as a free variable constrained to $SOF(N1) + SOF(N2) = 1.0$. Then the proton site was assigned according to the refinement results. The quality of high-pressure diffraction data for phase III at 1.0 GPa were clearly affected by the low quality of the crystal. This approximately ten times lowered the accuracy of the structural parameters, compared to the structure of low-temperature phase III (Supporting Information Table S3). For the structures of phase II at 0.60 GPa/296 K and X at 1.50 GPa/296 K, only the unit-cell parameters were determined. The selected crystal structure-refinement data are listed in Tables 1 and 2; complete

Table 1. Selected Crystal Data for High-Pressure Structures of DabcoHClO₄, All at 296(2) K

phase	II	III	X
pressure (GPa)	0.20(2)	1.00(2)	1.80(2)
crystal system	orthorhombic	orthorhombic	orthorhombic
space group	<i>Pm2₁n</i>	<i>Pc2₁n</i>	<i>Pc2₁b</i>
unit cell (Å)			
<i>a</i>	8.771(3)	8.496(4)	6.0197(11)
<i>b</i>	9.673(3)	9.4293(16)	12.929(3)
<i>c</i>	5.3402(12)	10.6475(13)	20.964(4)
Z/Z'	2/0.5	4/1	8/2
volume (Å ³)	453.1(2)	852.9(4)	1631.5(6)
D_{calcd} (g/cm ³)	1.551	1.656	1.731
final R_1/R_2 ($I > 2\sigma_1$)	0.0746/0.1744	0.1005/0.2092	0.0907/0.1682

experimental details are given in Tables S1 and S2 in the Supporting Information. The observation of increased unit cell of phase IV has been based on additional very weak reflections. Their intensity was too small for allowing atomic displacements to be determined. Similarly, the satellite reflections in phase V were so subtle that we could not reach reliable conclusions. On the other hand the occurrence of these phases was independently well documented by the DSC and dielectric measurements. The space group of phase IV has been determined from systematic absences of reflections combined with the dielectric-measurements information that it remains ferroelectric. Structural drawings were prepared using the X-Seed interface of POV-Ray.

Table 2. Selected Crystal Data for Low- and High-Temperature Structures of DabcoHClO₄, All at 0.1 MPa (cf. Table S2 in Supporting Information)

phase	I ^a	II	III	IV	V
T (K)	382.0(1)	253.0(1)	150.0(1)	114.5(1)	96.5(1)
crystal system	tetragonal	orthorhombic	orthorhombic	orthorhombic	orthorhombic
space group	<i>P4/mmm</i>	<i>Pm2₁n</i>	<i>Pc2₁n</i>	<i>Pc2a</i>	modulated
unit cell (Å)					
<i>a</i>	6.6786(10)	8.816(1)	8.667(2)	17.247(2)	17.255(1)
<i>b</i>	6.6786(10)	9.750(1)	9.744(2)	9.837(1)	39.395(3)
<i>c</i>	5.3694(10)	5.343(1)	10.680(2)	10.712(1)	10.719(1)
Z/Z'	1/0.25	2/0.5	4/1	8/2	32 ^b
volume (Å ³)	239.50(9)	459.30(11)	901.9(3)	1817.31	7286.40
D_{calcd} (g/cm ³)	1.471	1.535	1.565	1.554	1.550
R_1/R_2 ($I > 2\sigma_1$)	0.0323/0.0528	0.0324/0.0882	0.0343/0.0972		

^aRef 6. ^bZ' is not determined for this modulated structure.

3. DISCUSSION

3.1. DabcoHClO₄ Phases. The dabcoHClO₄ phases transform within the same lattice, where the corresponding crystal axes are either parallel or run along diagonals [110] and $[1\bar{1}0]$, as shown in Figure 7. To preserve the consistent direction of axis [z] in phase I with the [z] axes of other phases, unconventional settings of the space groups for phases II, III, IV, and X have been chosen.

Presently ten dabcoHClO₄ phases have been documented by dielectric, calorimetric, and X-ray diffraction methods at varied pressure and temperature conditions, as illustrated in the phase diagram in Figure 8. The determined dabcoHClO₄ phases I, II, III, and X have common structural features of the dabcoH⁺ cations NH⁺...N bonded into chains running along one direction [001], and the anions located close to the H-bonds. Moreover, the unit cells of all investigated phases I, II, III, IV, V and X can be expressed as multiples of the unit-cell dimensions of phase I, as illustrated in Figures 7 and S1 (letter "S" preceding the figure and table numbers indicate the Supporting Information). At ambient pressure, phase I (of tetragonal space group *P4/mmm*) is stable between 377 K and about 535 K when the compound starts decomposing; phase II, of orthorhombic space group *Pm2₁n*, is stable between 377 and 220 K; phase III, space group *Pc2₁n*, below 220 K; phase IV, space group *Pc2a*, below 117 K; phase V, orthorhombic modulated, below 105 K; and phases VI–IX below 95, 76, 56, and 47 K, respectively. High-pressure phase X was obtained above 1.50 GPa. In the structure of tetragonal phase I the ions are disordered about the 4-fold axis. The onset of halting their rotations induces the transition to orthorhombic phase II. In phases I and X the proton is disordered, and it is ordered in phases II and III. There are two symmetry-independent dabcoH⁺ and ClO₄⁻ ions in phase X. In phases II and low-temperature phase III the cations have similar conformation, with the N–C–C–N groups planar or nearly planar (their torsion angles are equal or close to 0°; Table S3 in the Supporting Information). However, in high-pressure phases III and X the diamineethylene moieties are slightly twisted all in one sense, so the cation assumes a so-called propeller conformation.

The crystal structures of phases I, II, III, and X have been fully solved, and the unit-cell dimensions have been measured for phases IV and V. The information about the boundaries of phases VI, VII, VIII, and IX is based on electric permittivity measurements (Figures 2 and 3), however the supramolecular

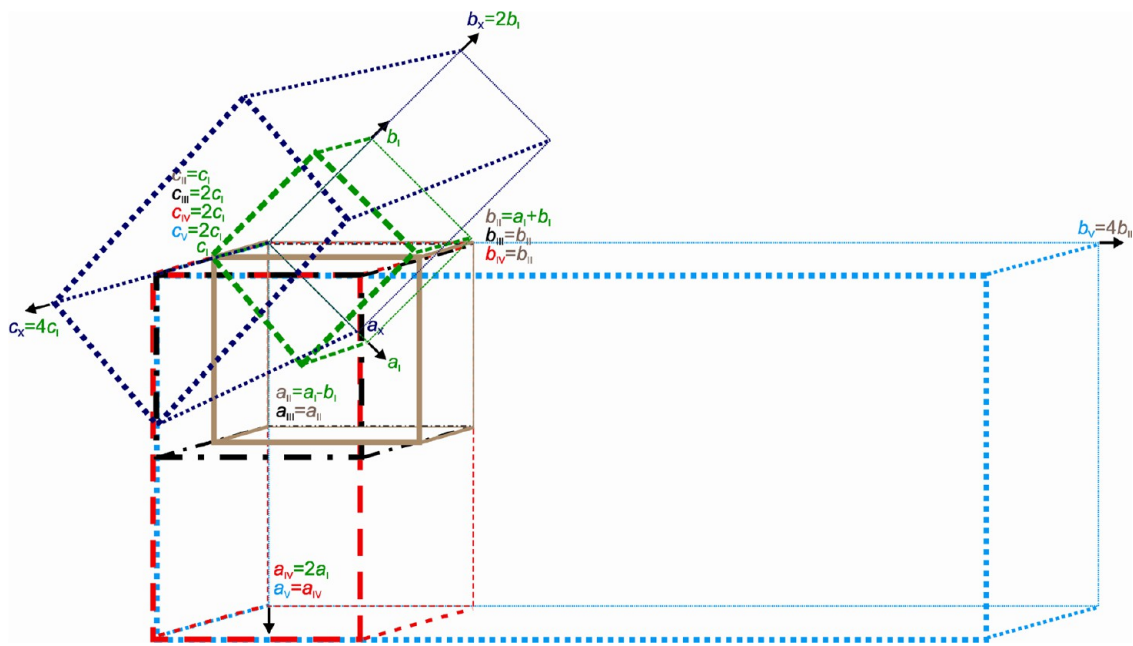


Figure 7. Unit-cell transformations between dabcoHClO₄ phases: I (green dashed lines), II (brown solid lines), III (black dotted and dashed lines), IV (red dashed lines), V (blue dotted lines), and X (navy-blue dotted lines). Approximate vector relations between the unit cells of different phases have been shown in the same color code as the drawings.

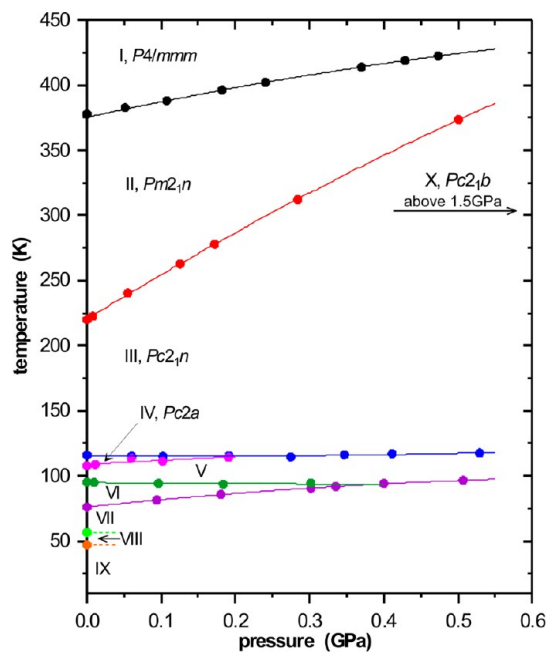


Figure 8. Low-pressure region of phase diagram of dabcoHClO₄. Solid lines have been drawn through the transition points determined by calorimetric and dielectric measurements. The diagram region has been shown only to 0.6 GPa for clarity (cf., Figure S2 in the Supporting Information the diagram is extended to 2.0 GPa).

structure of the NH⁺⋯N-bonded chains with anions between is highly unlikely to be destabilized. Thus it can be presumed that the low-temperature phases and the known dabcoHClO₄ phases are isostructural in their main features, and that they differ because of fine transformations, as discussed below.

3.2. Hydrogen Bonds Patterns. The NH⁺⋯N-bonded chains are linear in phase I, insignificantly distorted from linearity in phase II, slightly nonlinear in phase III, and

significantly wavy in phase X (Figure 9). These chains run along the [001] direction in phases I, II, III, and X, where the

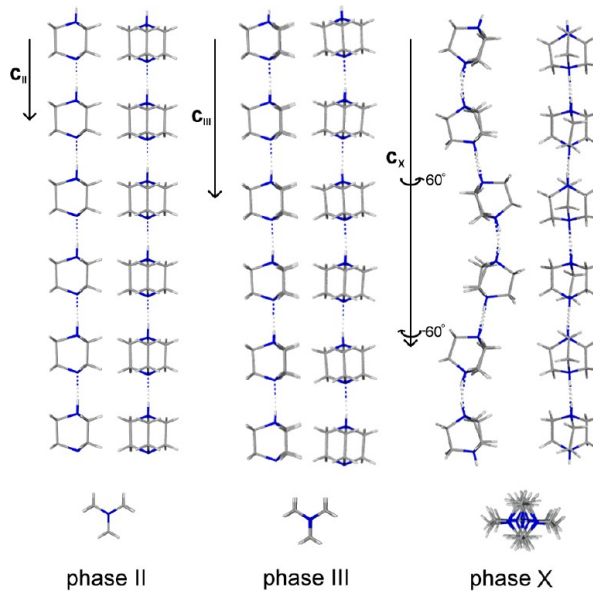


Figure 9. NH⁺⋯N bonded chains in dabcoHClO₄ phases II, III, and X viewed in two directions perpendicular (top left and right) and along (bottom) the chains. Arrows show the length of the crystal unit translation along [001] and the orientation changes of cations in phase X.

symmetry-independent chain interval contains one, two, two, and four amine groups (half, one, one, and two dabcoH⁺ cations), respectively. The distortion from linearity of the chains can be measured by the inclination angle between the direction of the chain and the line drawn through the nitrogen atoms of one cation. In phase II this inclination angle is from 0.3(2)° at 0.1 MPa/295 K to 0.7(2)° at 0.1 MPa/220 K and

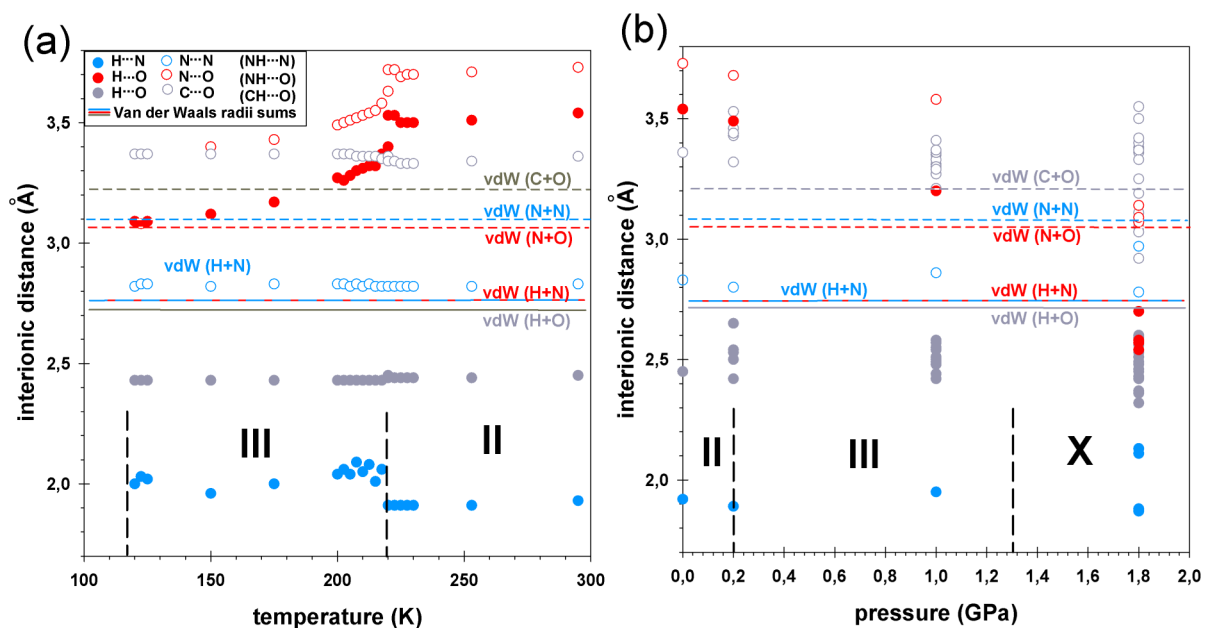


Figure 10. The shortest interionic distances in dabcoHClO_4 as a function of (a) temperature, and (b) pressure. Horizontal lines mark the sums of van der Waals (vdW) radii;²⁷ the solid ones for $\text{H}\cdots\text{N}$ (blue) and $\text{H}\cdots\text{O}$ (red and gray) and the dashed one for $\text{N}\cdots\text{N}$ (blue), $\text{N}\cdots\text{O}$ (red), and $\text{C}\cdots\text{O}$ (gray). The Roman numbers label the phases, and the vertical dashed lines indicate the boundaries between phases. Phase I has been omitted from these plots because of the extensive disorder in its structure.

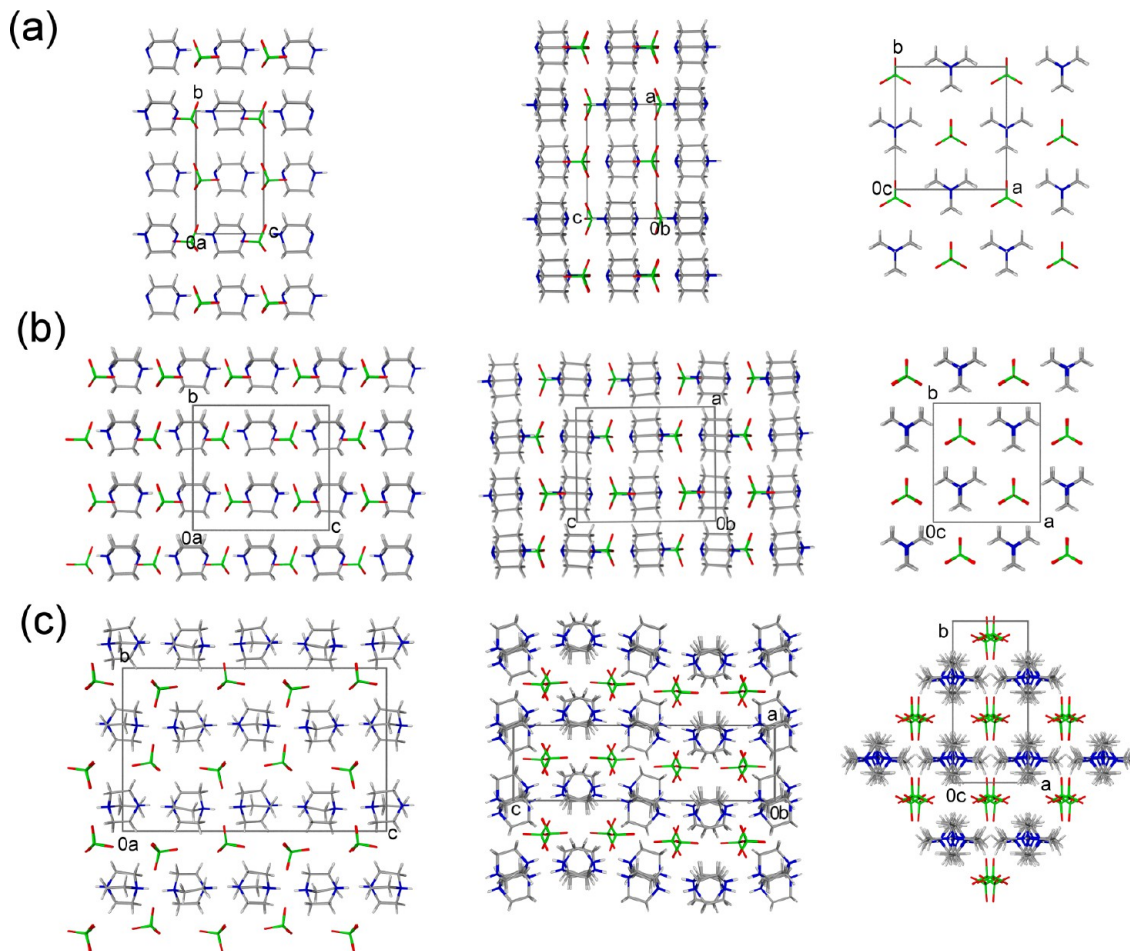


Figure 11. Crystal structures of dabcoHClO_4 phases: (a) II, (b) III, and (c) X, projected down the main crystal directions.

1(1)° at 0.20 GPa/296 K; in phase III it changes between 1.6(1)° at 0.1 MPa/220 K and 8.5(1)° at 0.1 MPa/120 K, and 15(1)° at 1.00 GPa/296 K. In phase X the dabcoH⁺ cations in the chain are tilted with respect to the [z] axis by 15.5(4)°.

In all these phases, there are short contacts between the ClO₄⁻ anions and hydrogen atoms of the ethylene bridges, and in high-pressure phase X also short NH⁺⋯O contacts are formed (Figure 10, Tables S4 and S5). In the high-pressure and low-temperature structures of phases II and III the NH⁺⋯O distances are much longer than the sums of corresponding van der Waals radii.²⁷ Generally, the shortening of CH⋯O distances is an expected result for compressed structures at high pressure. Moreover, it was demonstrated both spectroscopically²⁸ and structurally^{29–31} that high pressure favors the formation of CH⋯O, CH⋯N, CH⋯halogen hydrogen bonds. In all the structures of dabcoHClO₄ phases determined so far, the NH⁺⋯N bonding aggregation is predominant. However, the bending of the chains increasing with pressure can be associated with enhanced NH⁺⋯O interactions in phase X. The chain bending exposes the proton to its interactions with perchlorate anion located nearby.

The crystal packing in high-pressure phases of dabcoHClO₄ is presented in Figure 11. It is apparent that apart for the distortion of NH⁺⋯N bonded chains described above, there are clear differences between phases III and X in the orientation of cations and anions relative to the crystal directions. In all phases the anions are located close to the NH⁺⋯N bonds – the z-coordinates of the Cl atom and H⁺ are similar. In the xy plane there are four ClO₄⁻ anions around each NH⁺⋯N bond.

3.3. Dielectric Response. Except for the transition between phases I and II, all other transformations investigated in dabcoHClO₄ in this study proceed between ferroelectric phases. This information is apparent from the character of the observed dielectric anomalies, none of which resembles transformations between polar and nonpolar phases. Generally, the magnitude of dielectric response can arise from three main polarizability contributions: (i) electron; (ii) atomic/ionic; (iii) dipolar; and for ferroelectric phases (iv) a contribution from domain structure. The electron polarizability is independent of temperature, but the other types of polarizability can vary and differently contribute to the observed anomalies (Figures 2 and 3). It is difficult to evaluate the magnitudes of specific contributions (ii–iv) before more detailed information on the changes of phonon spectrum at phase transitions and the evolution of the ferroelectric domain structure is available.

4. CONCLUSIONS

At ambient pressure dabcoHClO₄ and dabcoHBF₄ are isostructural in their phases I and II. However, the phase behavior of these compounds in the low-temperature and high-pressure region is different. DabcoHClO₄ is much richer in low-temperature phases than dabcoHBF₄, for which only two low-temperature phases, phase III below 153 K and phase IV below 37 K, were identified.^{3,4,8} It appears that generally the mechanism of low-temperature phase transitions in dabcoHClO₄ is different than in dabcoHBF₄. The transition from dabcoHBF₄ phase II to phase III involves the protons disordering (reversely than expected from the temperature change) and the conformational transformation of the cations assuming the propeller conformation. In dabcoHClO₄, the ethylene bridges remain planar, and it is the tilts of cations and reorientations of anions which are responsible for lowering the structural symmetry. The origin of the differences between

dabcoHClO₄ and dabcoHBF₄ can be due to the different size, charge distribution, mass (98.455 vs 86.82 au, respectively), and moment of inertia of the ClO₄⁻ and BF₄⁻ anions, as well as different affinity to form (C/N)H⋯O and (C/N)H⋯F interactions. It was shown that high pressure promotes CH⋯O and CH⋯N interactions, very weak or nonexistent at 0.1 MPa.^{28,29} Weak interactions, including weak hydrogen bonds, are crucial for crystal packing and molecular aggregation^{31–34} and are often responsible for the formation of polymorphs of organic compounds at high pressure.^{35–37} It is also characteristic that the nonlinearity of chains increases with pressure. The bent NH⁺⋯N bonds allow the protons to increase its interactions NH⁺⋯O with the anion. None of the new dabcoHClO₄ structures determined in this study (phases III, IV and X) is isosymmetric with ferroelectric phase III of dabcoHBF₄^{1–4,8} nor with ferroelectric phase II of dabcoHReO₄.¹³ However, it is characteristic that all dabcoHClO₄ phases II, III, IV, and X remain polar and their structures are built of NH⁺⋯N bonded chains. In all these dabcoHClO₄ structures the polar direction is perpendicular to the chains.

■ ASSOCIATED CONTENT

📄 Supporting Information

Detailed crystallographic information on high-pressure phases (Table S1) and on low-temperature phases (Table S2), the torsion angles (Table S3), the shortest intermolecular interactions (Tables S4, S5), the unit-cell dimensions (Figure S1), and the phase diagram (Figure S2). This material is available free of charge via the Internet at <http://pubs.acs.org>.

■ AUTHOR INFORMATION

Corresponding Author

*E-mail: (A.K.) katran@amu.edu.pl. E-mail: (M.S.) masza@amu.edu.pl.

Notes

The authors declare no competing financial interest.

■ ACKNOWLEDGMENTS

A.O. acknowledges the reception of scholarship START from the Foundation for Polish Science in 2012. This study was supported by the Foundation for Polish Science, Team program 2009-4/6.

■ REFERENCES

- (1) Katrusiak, A.; Szafranski, M. *Phys. Rev. Lett.* **1999**, *82*, 576–579.
- (2) Szafranski, M.; Katrusiak, A. *Chem. Phys. Lett.* **2000**, *318*, 427–432.
- (3) Szafranski, M.; Katrusiak, A. *J. Phys. Chem. B.* **2004**, *108*, 15709–15713.
- (4) Budzianowski, A.; Katrusiak, A.; Szafranski, M. *J. Phys. Chem. B* **2008**, *112*, 16619–16625.
- (5) Szafranski, M.; Katrusiak, A.; McIntyre, G. J. *Phys. Rev. Lett.* **2002**, *89*, 215507 1–4.
- (6) Katrusiak, A. *J. Mol. Struct.* **2000**, *552*, 159–164.
- (7) Katrusiak, A.; Ratajczak-Sitarz, M.; Grech, E. *J. Mol. Struct.* **1999**, *474*, 135–141.
- (8) Szafranski, M. *J. Phys.: Condens. Matter.* **2004**, *16*, 6053–6062.
- (9) Szafranski, M.; Katrusiak, A. *J. Phys. Chem. B* **2008**, *112*, 6779–6785.
- (10) Olejniczak, A.; Katrusiak, A.; Szafranski, M. *Cryst. Growth Des.* **2010**, *10*, 3537–3546.
- (11) Budzianowski, A.; Katrusiak, A. *J. Phys. Chem. B* **2006**, *110*, 9755–9758.
- (12) Szafranski, M. *J. Phys. Chem. B* **2009**, *113*, 9479–9488.

- (13) Szafranski, M.; Katrusiak, A. *Phys. Rev. Lett.* **2012**, *109*, 169602–1–2.
- (14) Nowicki, W.; Olejniczak, A.; Katrusiak, A. *CrystEngComm*. **2012**, *12*, 6428–6434.
- (15) Dega-Szafran, Z.; Katrusiak, A.; Szafran, M.; Tykarska, E. *J. Mol. Struct.* **1999**, *484*, 49–61.
- (16) Paliwoda, D.; Dziubek, K. F.; Katrusiak, A. *Cryst. Growth Des.* **2012**, *12*, 4302–4305.
- (17) Zieliński, W.; Katrusiak, A. *Cryst. Growth Des.* **2013**, *13*, 696–700.
- (18) Merrill, L.; Bassett, W. A. *Rev. Sci. Instrum.* **1974**, *45*, 290–294.
- (19) Katrusiak, A. *Acta Crystallogr.* **2008**, *A64*, 135–148.
- (20) Piermarini, G. J.; Block, S.; Barnett, J. D.; Forman, R. A. *J. Appl. Phys.* **1975**, *46*, 2774–2780.
- (21) Mao, H. K.; Xu, J.; Bell, P. M. *J. Geophys. Res.* **1985**, *91*, 4673–4676.
- (22) *Xcalibur CCD System, CrysAlisPro Software System*, version 1.171.33; Oxford Diffraction Ltd.: Oxfordshire, U.K., 2004.
- (23) Budzianowski, A.; Katrusiak, A. *High-Pressure Crystallography*; Katrusiak, A., McMillan, P. F., Eds.; Kluwer: Dordrecht, the Netherlands, 2004, 101–112.
- (24) Katrusiak, A. *REDSHABS. Program for the Correcting Reflections Intensities for DAC Absorption, Gasket Shadowing and Sample Crystal Absorption*; Adam Mickiewicz University: Poznań, Poland, 2003.
- (25) Katrusiak, A. *Z. Krystallogr.* **2004**, *219*, 461–467.
- (26) Sheldrick, G. M. *Acta Crystallogr. A* **2008**, *64*, 112–122.
- (27) Bondi, A. *J. Phys. Chem.* **1964**, *68*, 441–451.
- (28) Chang, H.-C.; Jiang, J.-C.; Chuang, C.-W.; Lin, J.-S.; Lai, W.-W.; Yang, Y.-C.; Lin, S. H. *Chem. Phys. Lett.* **2005**, *410*, 42–48.
- (29) Dziubek, K.; Jęczyński, D.; Katrusiak, A. *J. Phys. Chem. Lett.* **2010**, *1*, 844–849.
- (30) Cai, W.; Katrusiak, A. *CrystEngComm*. **2011**, *13*, 6742–6746.
- (31) Cai, W.; Katrusiak, A. *CrystEngComm*. **2012**, *14*, 4420–4424.
- (32) Boldyreva, E. V. *CrystEngComm*. **2003**, *6*, 235–254.
- (33) Boldyreva, E. V.; Ivasheyskaya, S. N.; Sowa, H.; Ahsbahs, H.; Webwr, H.-P. *Z. Kristallogr.* **2005**, *220*, 50–57.
- (34) Boldyreva, E. V.; Naumov, D. Y.; Ahsbahs, H. *Acta Crystallogr. B* **1998**, *6*, 798–808.
- (35) Fabbiani, F. P. A.; Allan, D. R.; David, W. I. F.; Moggach, S. M.; Parsons, S.; Pulham, C. R. *CrystEngComm* **2004**, *6*, 504–511.
- (36) Oswald, I. D. H.; Chataigner, I.; Elphick, S.; Fabbiani, F. P. A.; Lennie, A. R.; Maddaluno, J.; Marshall, W. G.; Pulham, C. R.; Prior, T. J.; Smith, R. I. *CrystEngComm* **2009**, *11*, 359–366.
- (37) Boldyreva, E. V. *Cryst. Growth Des.* **2007**, *7*, 1662–1668.